Short communication

Relationship between Rayleigh wave polarization and state of stress

Michael Junge [a],[1], Jianmin Qu [b], Laurence J. Jacobs [a],[b],[*]

[a] *School of Civil and Environmental Engineering, Georgia Institute of Technology, Atlanta, Georgia 30332-0355, United States*
[b] *G.W. Woodruff School of Mechanical Engineering, Georgia Institute of Technology, Atlanta, Georgia 30332-0405, United States*

Abstract

This research develops an analytical model (using Stroh's formalism) to predict the affect of applied stress on the wave speed and the polarization of Rayleigh surface waves. Simulation results are then used to demonstrate that the polarization of a Rayleigh wave (which is reference-free) could be more sensitive than wave speed as an indicator of the state of stress.
© 2006 Elsevier B.V. All rights reserved.

PACS: 43.35.Cg; 43.35.Pt

1. Introduction and analytical model

The acoustoelastic effect – the dependency of ultrasonic wave speed on state of stress – is a well established phenomenon that has been extensively reported in the literature [1,2]. Application of this technique to measure applied or residual stress requires measurement of the wave speed by time-of-flight, so these measurements are not reference-free; the distance between the source and the receiver of the ultrasonic wave has to be known exactly. In contrast, this research provides the theoretical development of a reference-free, alternative technique by demonstrating that the polarization of a Rayleigh surface wave – defined as the ratio between the maximum in-plane, and the maximum out-of-plane displacement components – is directly related to the state of stress.

The acoustoelastic effect on Rayleigh waves in a homogeneous material was investigated by Hirao et al. [3] – they present the dispersion relationship of a Rayleigh wave in a

beam in bending. Duquennoy et al. also used Rayleigh waves to investigate residual stresses [4,5].

Three different states of a body are considered in this work, and each of these states must be carefully distinguished. A body that is in a totally stress- and strain-free state is said to be in the *natural state*. In reality, this state almost never exists in a real material because there are residual stresses or stresses due to load or fabrication processes, so the second state is called the *initial state*. An ultrasonic wave superimposes a further displacement, and causes another change in stress and strain – the resulting state is called the *final state*. Fig. 1 shows the position of a single particle for each of the different states. Following the convention proposed in [6], the position of a particle in the natural, initial and final states are referred to by the vectors ξ, X and x, respectively, and all these vectors are written in terms of the same Cartesian coordinate system. The displacements that result from the change of state are defined as: $u^i(\xi) = X - \xi$; $u^f(\xi) = x - \xi$; and $u(\xi) = x - X = u^f - u^i$.

The proposed solution approach uses Stroh's formalism [7], a mathematically elegant technique that has been used to solve two-dimensional, anisotropic elasticity problems and steady state problems. The idea of Stroh's formalism is to represent the solution of a problem in matrix-notation, then start with an initial assumed solution of the

---

[*] Corresponding author. Address: School of Civil and Environmental Engineering, Georgia Institute of Technology, Atlanta, Georgia 30332-0355, United States. Tel.: +1 404 894 2771; fax: +1 404 894 0211.
    E-mail address: laurence.jacobs@ce.gatech.edu (L.J. Jacobs).
[1] Current address: Institute of Applied and Experimental Mechanics, University of Stuttgart, Stuttgart, Germany.
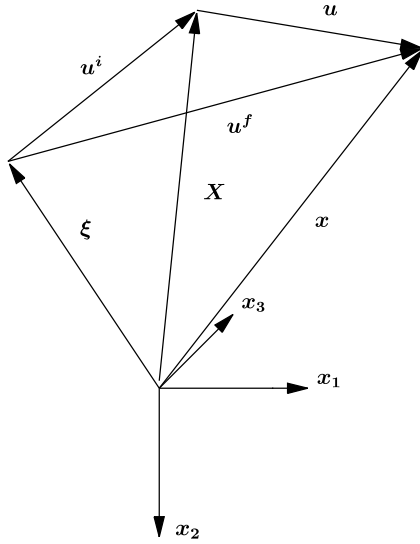
Fig. 1. Coordinates for a material point in the natural (ξ), initial (X) and final (x) states, following [6].

displacements, and then derive the stresses with this assumed solution. Following [8–10], the equations of motion in a solid with initial homogeneous stress are

$$(\delta_{IK} t^i_{JL} + \widehat{C}_{IJKL})\frac{\partial^2 u_K}{\partial X_J X_L} = \rho^0(1 - \varepsilon^i_{NN})\frac{\partial^2 u_I}{\partial t^2}, \tag{1}$$

where $\boldsymbol{t}^i$ is the Cauchy stress tensor (state of stress at a material point as a function of X) and $\boldsymbol{\varepsilon}^i$ is the initial (linear) strain tensor. Since the mass density changes due to deformation (and mass must be conserved), Eq. (1) uses the fact that for small deformations, the density can be approximated by $\rho^i \approx \rho^0(1 - \varepsilon^i_{NN})$. Finally note that for an isotropic material, $\widehat{\boldsymbol{C}}$ can be expressed as

$$\begin{aligned}\widehat{C}_{IJKL} &= \lambda\delta_{IJ}\delta_{KL} + \mu(\delta_{IK}\delta_{JL} + \delta_{IL}\delta_{JK}) + [(-\lambda + v_1)\delta_{IJ}\delta_{KL} \\ &\quad + (-\mu + v_2)(\delta_{IK}\delta_{JL} + \delta_{IL}\delta_{JK})]\varepsilon^i_{MM} \\ &\quad + 2(\lambda + v_2)(\varepsilon^i_{IJ}\delta_{KL} + \varepsilon^i_{KL}\delta_{IJ}) \\ &\quad + 2(\mu + v_3)(\varepsilon^i_{IK}\delta_{JL} + \varepsilon^i_{IL}\delta_{JK} + \varepsilon^i_{JK}\delta_{IL} + \varepsilon^i_{JL}\delta_{IK}), \end{aligned} \tag{2}$$

where μ and λ are the well known Lamé constants and v_i, $i = 1, 2, 3$ are the third-order elastic constants (TOE-constants) in the notation of [2]. It is important to note that even though this development uses a non-linear stress–strain relationship, displacements are assumed to be small, so only terms that are linear in either the gradient of $\boldsymbol{u}$ or $\boldsymbol{u}^i$ are retained.

Assume a wave that propagates in the X_1 direction and has a displacement that decays exponentially with depth (the X_2 direction)

$$\boldsymbol{u} = \boldsymbol{a}\mathrm{e}^{\mathrm{i}k(X_1 + pX_2 - c_r t)}, \tag{3}$$

where $\boldsymbol{a}$ is the displacement amplitude vector, k the wavenumber, p the decay parameter and c_r the Rayleigh wave speed. Substitution of Eq. (3) into Eq. (1) yields

$$\begin{aligned}\{(\delta_{IK} t^i_{22} + \widehat{C}_{I2k2})p^2 &+ (\delta_{IK} t^i_{12} + \widehat{C}_{I1K2} + \delta_{IK} t^i_{21} + \widehat{C}_{I2K1})p \\ &+ (\delta_{IK} t^i_{11} + \widehat{C}_{I1K1}) - \delta_{IK}\rho^0(1 - \varepsilon^i_{NN})c_r^2\}a_K = 0. \end{aligned} \tag{4}$$
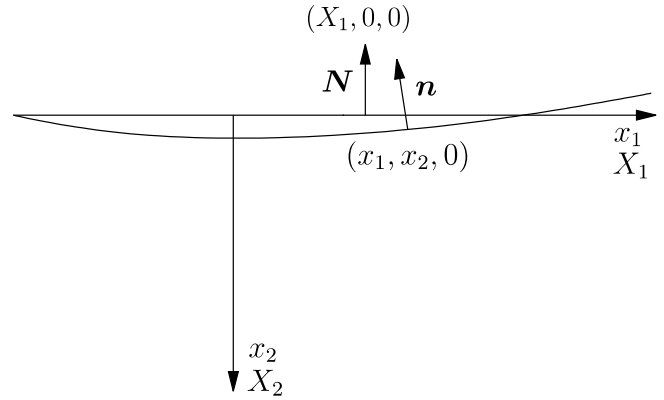

Fig. 2. Boundary conditions for a Rayleigh wave in a predeformed half-space.

For the case of constant initial stress, the surface is taken to be stress free in both the initial and the final states, so following Fig. 2, the boundary conditions are expressed as

$$N_J t^i_{IJ} = 0, \quad \text{at } X_2 = 0, \tag{5}$$

$$n_j t^f_{ij} = 0, \quad \text{on the wavy surface.} \tag{6}$$

These two boundary conditions can be combined, by first transforming the Cauchy stress tensor ($\boldsymbol{t}^f$, that refers to the final state) to an incremental Kirchhoff stress tensor, $\boldsymbol{T}$, as well as transforming the unit normal, $\boldsymbol{n}$ to $\boldsymbol{N}$, and applying $N_J = \begin{bmatrix} 0 & -1 & 0 \end{bmatrix}$. Eq. (6) can then be expressed as

$$T_{I2} = \widehat{C}_{I2KL}\frac{\partial u_K}{\partial X_L} = 0, \quad \text{at } X_2 = 0. \tag{7}$$

Since the stress tensor $\boldsymbol{t}^i$ is assumed to be constant and t^i_{22} and t^i_{12} have to be zero at the surface due to Eq. (5), these stress components are zero everywhere. Eq. (4) can then be written in a more compact form

$$\underbrace{\{p^2\widehat{\boldsymbol{S}} + p(\widehat{\boldsymbol{R}} + \widehat{\boldsymbol{R}}^T) + \widehat{\boldsymbol{Q}} - \rho^0(1 - \varepsilon^i_{NN})c_r^2\boldsymbol{I}\}}_{\boldsymbol{D}(c_r, p)}\boldsymbol{a} = 0 \tag{8}$$

with $\widehat{S}_{IK} = \widehat{C}_{I2K2}$, $\widehat{R}_{IK} = \widehat{C}_{I1K2}$, $\widehat{Q}_{IK} = \delta_{IK} t^i_{11} + \widehat{C}_{I1K1}$, and $\boldsymbol{I}$ is the identity matrix. For a non-trivial solution of this homogeneous equation, the matrix $\boldsymbol{D}$ must have a rank deficiency, thus

$$\|\boldsymbol{D}(c_r, p)\| = 0. \tag{9}$$

The solution of Eq. (9) yields three pairs of complex conjugate roots for p (for a given c_r). It is physically reasonable to select only those roots that have displacements that decrease, for an increasing X_2. Thus, the roots with a negative imaginary part are discarded. The roots with positive real parts are denoted with p_n, $n = 1, 2, 3$. It is worth noting that for this problem, all values of p_i are purely imaginary [7]. The displacement amplitude vector, $\boldsymbol{a}_i$, for each p_i can be determined by solving for the null-space of $\boldsymbol{D}$. This allows

the displacement to be written as a linear combination of the single solutions using the matrix-notation, or

$$\boldsymbol{u} = \boldsymbol{AG}(X_2)\boldsymbol{f} \; e^{ik(X_1 - c_r t)}, \tag{10}$$

where

$$\boldsymbol{A} = [\boldsymbol{a}_1, \quad \boldsymbol{a}_2, \quad \boldsymbol{a}_3] \tag{11}$$

$$\boldsymbol{G}(X_2) = \begin{bmatrix} e^{ikp_1 X_2} & 0 & 0 \\ 0 & e^{ikp_2 X_2} & 0 \\ 0 & 0 & e^{ikp_3 X_2} \end{bmatrix} \tag{12}$$

and $\boldsymbol{f}$ is an vector whose elements are the factors for the linear combination. The vector $\boldsymbol{f}$ will be determined by applying the boundary conditions – plug Eq. (10) into the boundary conditions, Eq. (7), yielding

$$\underbrace{(\widehat{\boldsymbol{R}}^T \boldsymbol{A} + \widehat{\boldsymbol{S}} \boldsymbol{A} \boldsymbol{P})}_{\boldsymbol{B}(c_r, p)} \boldsymbol{f} = 0 \tag{13}$$

with

$$\boldsymbol{P} = \begin{bmatrix} p_1 & 0 & 0 \\ 0 & p_2 & 0 \\ 0 & 0 & p_3 \end{bmatrix}. \tag{14}$$

The condition of a non-trivial solution to Eq. (13) gives

$$\|\boldsymbol{B}(c_r, p)\| = 0. \tag{15}$$

The vector $\boldsymbol{f}$ is then obtained by solving for the null-space of $\boldsymbol{B}(c_r, p)$.

The speed c_r that satisfies Eqs. (9) and (15) is the wave speed of the Rayleigh wave in a prestressed body. The displacements are then determined with Eq. (10), and the polarization vector is given by $\hat{\boldsymbol{u}}(X_2) = \boldsymbol{AG}(X_2)\boldsymbol{f}$. The polarization is calculated using the maximum displacements in the X_1 and X_2 directions. At the surface ($X_2 = 0$), the polarization, $\boldsymbol{\Pi}$, is given by

$$\boldsymbol{\Pi} = \frac{(\boldsymbol{Af})_1}{(\boldsymbol{Af})_2}. \tag{16}$$

Unfortunately, there is not an easy analytical solution for this problem and an iterative algorithm for the numerical solution of Eq. (16) is described in [9].

2. Numerical results and discussion

Consider two materials, mild steel and polystyrene, under an uniaxial stress, t_{11}^i that varies between ±25 MPa. Changes in Rayleigh wave speed and polarization will be very small, so consider relative changes in wave speed and polarization (e.g., $\Delta\Pi = (\Pi - \Pi_0)/\Pi_0$, where the subscript 0 denotes the polarization in the natural state). The simulation results for mild steel are shown in Fig. 3(a), and for polystyrene in Fig. 3(b) with the mass density, Lamé constants, and TOE-constants used given in Table 1. Fig. 3(a) shows an approximately linear (inversely) proportional relationship between relative change in
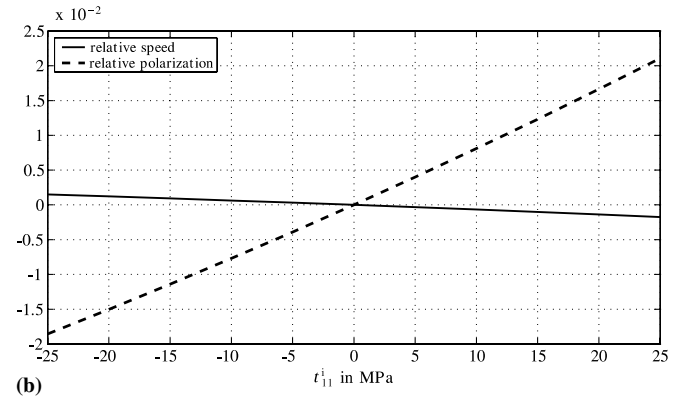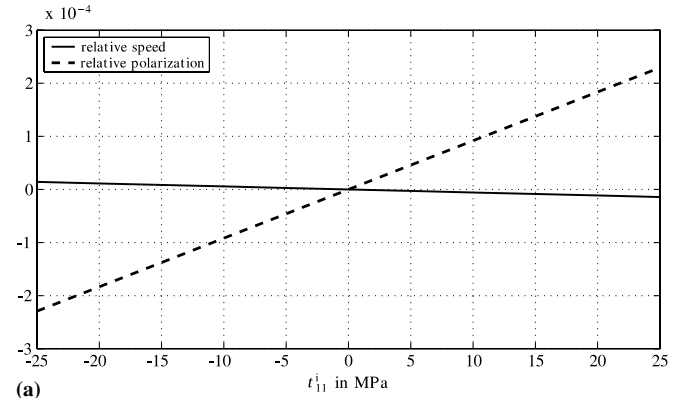

Fig. 3. Relative change in wave speed and polarization as a function of applied uniaxial stress t_{11}^i along the propagation direction: (a) mild steel and (b) polystyrene.

Table 1
Mass density, Lamé constants and the TOE-constants of the simulated materials

Material	ρ (kg/m³)	λ (GPa)	μ (GPa)	v_1 (GPa)	v_2 (GPa)	v_3 (GPa)
Mild steel	7837.0	107.4	81.9	−13.0	−200.0	−200.0
Polystyrene	1040.0	2.8	1.3	−18.9	−13.3	−10.0

Rayleigh wave speed, Δc_r, and applied uniaxial stress. This relationship is $\Delta c_r = k_{\text{steel}}^c \cdot t_{11}^i$, where k_{steel}^c is a proportionality factor of -5.7×10^{-7}/MPa. Fig. 3(a) also presents the change in relative polarization, and this change in polarization is an order of magnitude higher than the relative change of wave speed. Again, there is also an approximately linear relationship given by $\Delta\Pi = k_{\text{steel}}^p \cdot t_{11}^i$ with $k_{\text{steel}}^p = 9.81 \times 10^{-6}$/MPa. Fig. 3(b), shows the two proportionality factors for polystyrene, k_{PS}^c and k_{PS}^p. There is no longer an "exact" linear relationship between relative change in wave speed and t_{11}^i (and between relative polarization and t_{11}^i), but the approximated linear proportionality factors k_{PS}^c and k_{PS}^p indicate that the polarization is again an order of magnitude more sensitive to stress than wave speed. Finally, Fig. 4 shows the changes of the "orbit" of a particular particle on the surface, for a change in stress from +25 to −25 MPa.

Five other materials are analyzed and the results are summarized in Table 2. First note that the proportionality
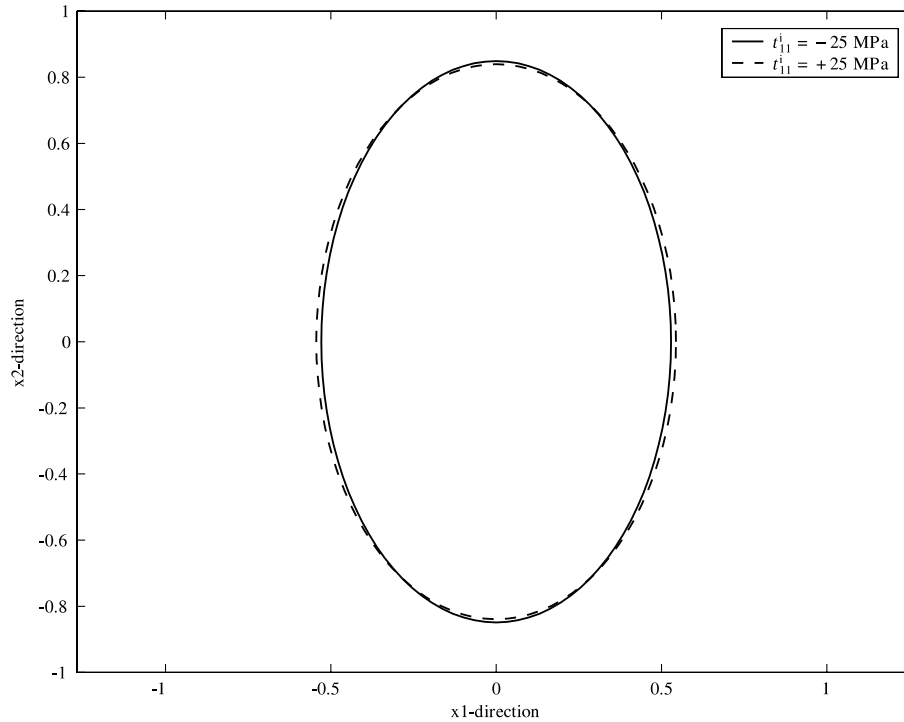
Fig. 4. Trajectory plot: motion of a particle on the surface in polystyrene. Solid line shows motion for uniaxial compression, dashed line represents uniaxial tension.

Table 2
Comparison of the simulation results for the different materials

Material	$k^c = \Delta c_r/c_{r0}$ (1/MPa)	Pol-change k^p (1/MPa)	Ratio k^p to k^p_{steel}	Ratio of k^p to k^c
Mild steel	−5.7217E-07	9.1822E-06	1.00	−16.05
Al (99.3%)	−1.0023E-05	3.5809E-05	3.90	−3.57
Al alloy B53S	−2.8842E-06	2.7893E-05	3.04	−9.67
Al alloy D54S	−2.0447E-05	6.6730E-05	7.27	−3.26
Al alloy JH77S	−2.3684E-05	6.0955E-05	6.64	−2.57
Polystyrene	−6.4805E-05	7.9229E-04	86.29	−12.23
Brass	−6.4805E-06	3.8480E-05	4.19	−5.94

Values are changes per MPa applied stress.

factor of the relative polarization, k^p, is larger than the proportionality factor of the relative wave speed, k^c, for all materials. For mild steel, Al-B53S and polystyrene, k^p is an order of magnitude larger than k^c. The fourth column shows the ratio between the proportionality factor of the polarization of steel, k^p_{steel}, and the proportionality factors of the various other materials. These results lead to the following conclusion – the stronger the material, the smaller are the changes in both wave speed and polarization. In summary, determination of t^i by the measurement of the polarization should be more sensitive than the determination of t^i by the measurement of the wave speed for these materials.

Finally consider the sensitivity of these results to uncertainties in the values of the TOE-constants – it is well established that the TOE-constants will have a large degree of scatter [11]. A simulation is implemented to calculate this dependency, by examining the proportionality factors, k^c

and k^p, as a function of the TOE-constants. Note that the Lamé constants of a material can be determined very precisely (with an error less than 1%), so their values are assumed to be constant throughout this simulation. Mathematically, the variation of the TOE-constants spans a three-dimensional space, and has the shape of a cube [9]. The simulation results show that there is a strictly monotonic relationship between each of the TOE-constants, and the proportionality factors k^c and k^p. Fig. 5 shows the results of assuming an uncertainty of 20% in the TOE-constants of aluminum B53S, and the relative wave speed and the relative polarization changes within the grey shaded regions; it is clear that the polarization results are less dependent on knowing the exact values of the TOE-constants. Overall, the relative polarization is *more sensitive* to applied stress than the relative wave speed (since the proportionality factor, k^p, is larger than k^c), while being less sensitive to uncertainties in the values of the TOE-constants.

It is important to note that this study did not investigate the influence of a number of critical factors including (but not restricted to) anisotropic texture and surface roughness. Further research is needed to determine the influence of these factors on the relative polarization and thus show its robustness as an indicator of the state of stress – is polarization less sensitive than wave speed to these intrinsic material variations that could be present in a real material? This additional research is needed to demonstrate the effectiveness of Rayleigh wave polarization as a practical tool to measure applied or residual stresses.
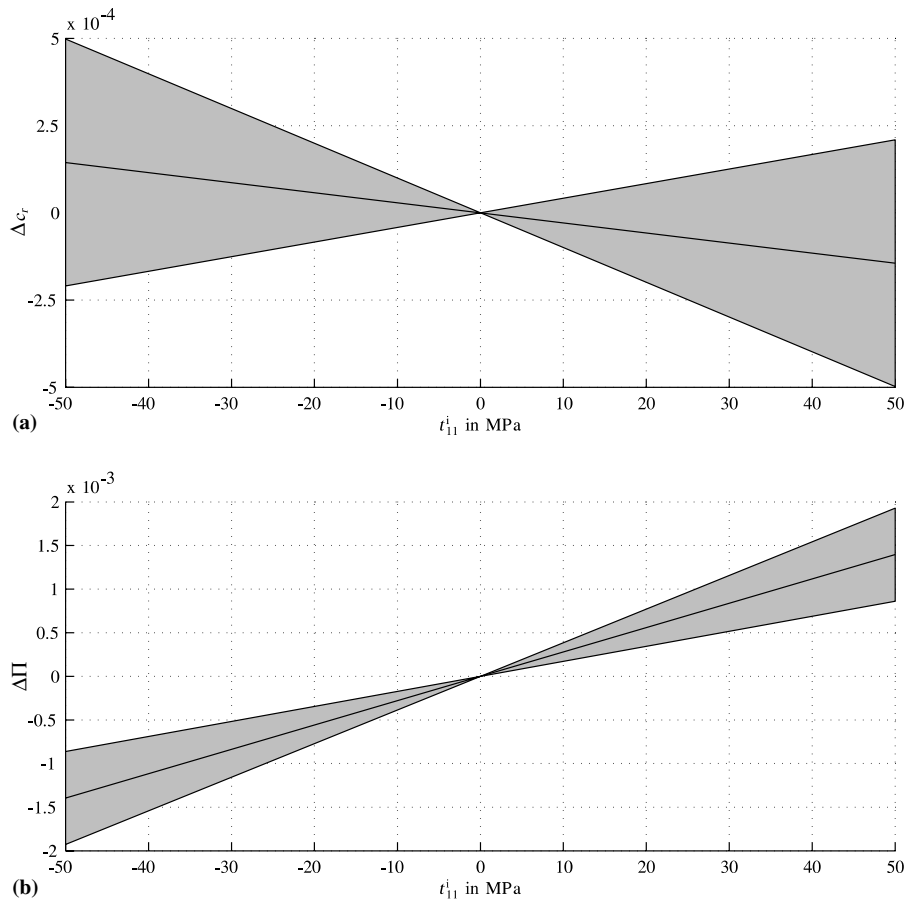
Fig. 5. Effect of uncertainties in the TOE-constants on the relative wave speed and relative polarization. If an uncertainty of 20% in the TOE-constants is assumed the relative wave speed and the relative polarization changes within the grey shaded area.

References

[1] D.I. Crecraft, Ultrasonic wave velocities in stressed nickel steel, Nature 195 (4847) (1962) 1193.

[2] R.A. Toupin, B. Bernstein, Sound waves in deformed perfectly elastic materials. Acoustoelastic effect, Journal of the Acoustical Society of America 33 (2) (1961) 216–225.

[3] M. Hirao, H. Fukuoka, K. Hori, Acoustoelastic effect of Rayleigh surface wave in isotropic material, Journal of Applied Mechanics 48 (1981) 119–124.

[4] M. Duquennoy, M. Ouaftough, M. Ourak, Ultrasonic evaluation of stress in orthotropic materials using Rayleigh waves, NDT & E International 32 (4) (1999) 189–199.

[5] M. Duquennoy, M. Ouaftough, M.L. Qian, M. Ourak, Ultrasonic evaluation of stress in orthotropic materials using Rayleigh waves, NDT & E International 34 (5) (2001) 355–362.

[6] Yih-Hsing Pao, Wolfgang Sachse, Hidekazu Fukuoka, Acoustoelasticity and ultrasonic measurements of residual stresses, Physical Acoustics 17 (1984) 61–143.

[7] A.N. Stroh, Steady state problems in anisotropic elasticity, Journal of Mathematics and Physics 41 (1962) 77–103.

[8] J.D. Achenbach, Wave Propagation in Solids, eighth ed., Elsevier Science Publishers B.V., 1999.

[9] Michael Junge. Measurement of applied stresses using the polarization of Rayleigh waves. Master's thesis, School of Civil and Environmental Engineering, Georgia Institute of Technology, August, 2003.

[10] Thomas C.T. Ting, Anisotropic Elasticity, Oxford University Press, 1996.

[11] R.T. Smith, R. Stern, R.W.B. Stephens, Third-order elastic moduli of polycrystalline metals from ultrasonic velocity measurements, Journal of the Acoustical Society of America 40 (5) (1966) 1002–1008.